

Secondary-side-only Simultaneous Power and Efficiency Control for Two Converters in Wireless Power Transfer System

Giorgio Lovison, Motoki Sato*, Takehiro Imura and Yoichi Hori

The University of Tokyo / * Toyo Denki Seizo K.K.

5-1-5 Kashiwanoha, Kashiwa, Chiba, 277-8561, Japan / * 3-8 Fukuura, Yokohama, Kanagawa, 236-0004, Japan

Email: lovison@hflab.k.u-tokyo.ac.jp, satoum@hflab.k.u-tokyo.ac.jp, imura@hori.k.u-tokyo.ac.jp, hori@k.u-tokyo.ac.jp

Abstract – Electric vehicles (EVs) are very useful but suffer from limited range and long battery charge time. Using wireless power transfer (WPT) allows these issues to be solved. In WPT, the control of the power converters is very important in order to achieve high efficiency and be able to extract the desired power from the source at any time. Until now, it was possible to perform either power control or efficiency control in the secondary side, but not both at the same time. Therefore, the authors propose a novel control for power and efficiency with two converters entirely performed on the secondary side of the wireless system, independently from the primary side. The proposed control allows achieving high transmitting efficiency for the desired power by means of a half active rectifier. Simulations and experiments shows that this method effectively allows achieving high efficiency even when the desired power is varied.

Keywords— *Half active rectifier, secondary side control, wireless power transfer, efficiency control, power control.*

I. INTRODUCTION

In recent years, electric vehicles have been a main research topic. Using an electric motor for traction, they have several advantages with respect to conventional vehicles fuelled by gasoline such as low environmental impact, fast response, high torque delivery to the wheels and reduction of noise pollution. On the other hand, they have some issues, most notably limited cruising range, long battery charge time and higher cost.

With wireless power transfer (WPT) via magnetic resonant coupling [1] it is possible to overcome these problems. In fact, when applied to an electric vehicle, WPT allows battery charging of the electric vehicle while in motion as well as while stationary. Magnetic resonance coupling guarantees robustness against misalignment, increased air gap and higher transmission efficiency when compared to conventional induction method. The difference between these two methods lies in the compensation by means of capacitances, like a series-series (SS)

compensation circuit. However, an optimal power transmission requires a good converter control to minimize losses while delivering the desired power to the load [2]. The most used types of control are power control and efficiency control and they are to be carried on either the wireless power system primary side [3][4], on the secondary side [5][6] or on both sides [7][8]. In a wireless power transfer system for battery charging, the secondary side include a rectifier and a DC/DC converter connected to the load, a battery. Therefore, it is possible to control the efficiency and the power flow only with the converters in the secondary side. However, until now, power and efficiency control have been performed in different sides of the systems (e.g. efficiency control on primary side and power control on secondary side). A novel control able to transfer the desired power with high efficiency on the receiving side is desirable. Therefore, in this paper, the authors propose a power and efficiency control for the secondary side of a WPT system with SS compensation.

More in detail, this paper is organized as following. Section II explains the case of study. Section III presents how the power and efficiency characteristics of WPT secondary side are related to the load impedance while section IV explains the concept of the proposed control. Section V illustrates the control operation and the choice of operation points and section VI discuss the simulation and experimental results. Section VII finally draws the conclusions from the results and suggests the future works.

II. CASE OF STUDY

This study focuses on the secondary side of a wireless power transfer system with SS compensation: it includes a half active rectifier (HAR), a DC/DC converter and a battery as load. The frequency adopted in the wireless system is the resonant frequency given by the coil parameters, which are independent from the load and the distance between the coils. The resonant angular frequency is given as follows:

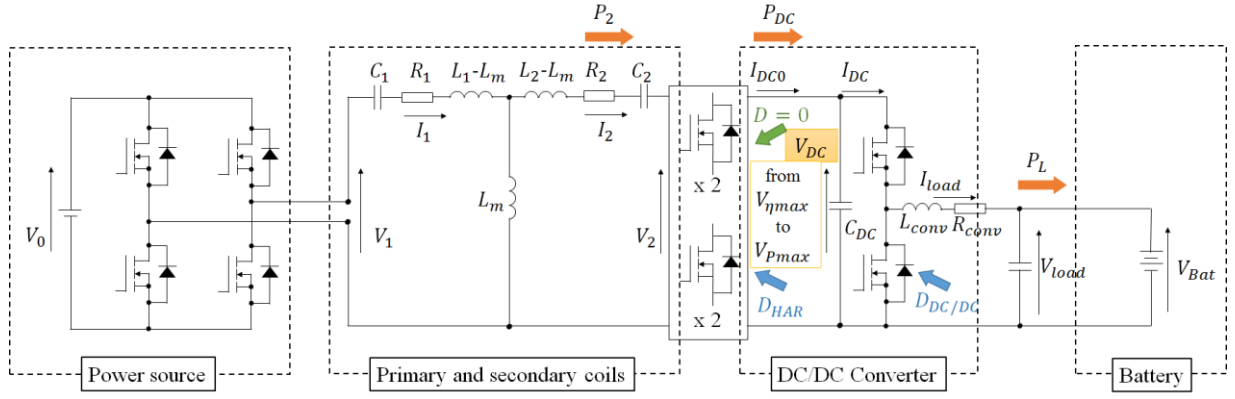


Figure 1: Reference circuit of WPT using SS compensation and equivalent coil configuration.

$$\omega = \sqrt{\frac{1}{L_1 C_1}} = \sqrt{\frac{1}{L_2 C_2}} \quad (1)$$

with L_1 and C_1 as the primary coil inductance and capacitance, respectively; similarly, L_2 and C_2 are the secondary coil inductance and capacitance. The coil internal resistance has no effect on the resonant frequency but affects the losses and the dynamic response of the system. The mutual inductance between the primary and secondary coil depends on the distance between them. The values of these circuit parameters are listed in table 1. In [11] the relationship between the coil inductance and the mutual inductance is explained. In figure 1 finally is shown the reference circuit, where after the HAR there is a DC/DC converter and then the load. This is a constant voltage load (i.e. battery) to be supplied with a constant power to avoid oscillations that decrease the efficiency.

Therefore, the author proposes to use a HAR paired with a DC/DC converter to control the efficiency and the power flow in the secondary side only. The HAR and the DC/DC converter operate independently from the primary side converters. The motivation to control only the secondary side is to keep the control simple by not employing any kind of communication with the primary side (e.g. Bluetooth) in order to have an easier system to model.

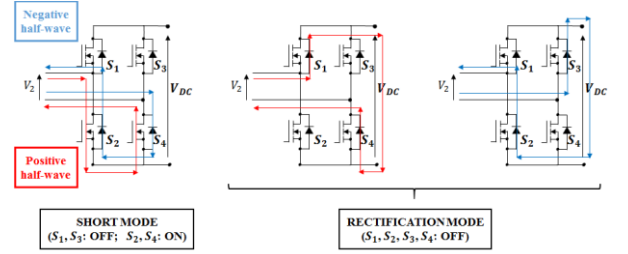


Figure 2: HAR modes.

III. POWER AND EFFICIENCY CHARACTERISTICS OF WPT

In WPT theory, the formulae of the load power P_L and transmitting efficiency η , presented in previous papers such as [9],[10] and [11], are given respectively by:

$$P_L = \frac{(\omega L_m)^2 Z_L}{[R_1(Z_L + R_2) + (\omega L_m)^2]^2} V_{1,0}^2 \quad (2)$$

$$\eta = \frac{(\omega L_m)^2 Z_L}{(R_2 + Z_L)[R_1(Z_L + R_2) + (\omega L_m)^2]} \quad (3)$$

where Z_L is the load impedance, R_2 is the secondary coil resistance, R_1 is the primary coil resistance, L_m is the mutual inductance between the coils and $V_{1,0}$ is the rms value of the fundamental wave of primary side voltage. In this paper, the power factor of the primary side voltage is assumed to be unity, therefore the power factor of the fundamental wave of the secondary side voltage V_2 is considered to be unity, too. The presence of SS compensation makes the secondary side coil operate like an equivalent current source, so the secondary side voltage V_2 is a square wave. The HAR is structured like a full wave diode bridge whose low side diodes are replaced by active devices like MOSFETs or IGBTs: by turning on the both the devices on the low side, the coil terminals are shorted (short mode) and no power is transmitted to the load. This is

TABLE I. EXPERIMENTAL PARAMETERS OF THE CIRCUIT

Parameter	Value
Battery voltage [V]	6.34
Primary coil capacitance C_1 [nF]	6.03
Secondary coil capacitance C_2 [nF]	12.15
DC link capacitor C_{DC} [mF]	1
Primary coil inductance L_1 [μ H]	417.8
Secondary coil inductance L_2 [μ H]	208.5
Mutual inductance L_m [μ H]	39.2
Coil gap [mm]	100
Resonant frequency [kHz]	100
Primary coil resistance R_1 [Ω]	1.83
Secondary coil resistance R_2 [Ω]	1.281

possible only because the SS compensation of magnetic resonant coupling makes the secondary side coil behave like an equivalent current source. On the other hand, if both the low side devices are off, the converter works like a conventional single-phase rectifier composed by diodes (rectification mode), as shown in figure 2, and power is sent to the load.

The influence of load impedance has been examined in [9], [10] and [12]. In particular, the load impedance associated with maximum transmission efficiency and the one related to maximum deliverable power are different. The former one is equal to:

$$Z_{L,\eta \max} = \sqrt{\frac{R_2}{R_1} (\omega L_m)^2 + R_2^2} \quad (4)$$

The voltage that maximizes the transmission efficiency can be expressed by:

$$V_{\eta \max} = \sqrt{\frac{R_2}{R_1}} \frac{\omega L_m}{\sqrt{R_1 R_2} + \sqrt{R_1 R_2 + (\omega L_m)^2}} V_{1,0} \quad (5)$$

On the other hand, the load impedance and the voltage related to the maximum available power are given by:

$$Z_{L,P \max} = \frac{(\omega L_m)^2}{R_1} + R_2 \quad (6)$$

$$V_{P \max} = \frac{\omega L_m}{2R_1} V_{1,0} \quad (7)$$

Voltages in (5) and (7) are rms values since the active power delivered to the load is related to the fundamental wave of the HAR input voltage, which is a square wave. Finally, in order to achieve the required power with high transmission efficiency, the total input impedance seen from the secondary coil must be a value between $Z_{L,\eta \max}$ and $Z_{L,P \max}$. By applying this concept to the secondary side system, the control of the input impedance allows to use the HAR to send the power desired by the load to the DC/DC converter, which in turn is used to ensure maximum transmitting efficiency. Figure 3 shows the relationship between power and efficiency with respect to the load impedance.

IV. PROPOSED CONTROL CONCEPT

As highlighted in figure 3, the power corresponding to maximum transmitting efficiency is fixed. However, by the proposed secondary side control, it is possible to send a different power value while retaining the same transmitting efficiency. This is because of the switching between short mode and rectification mode by HAR. The length of the

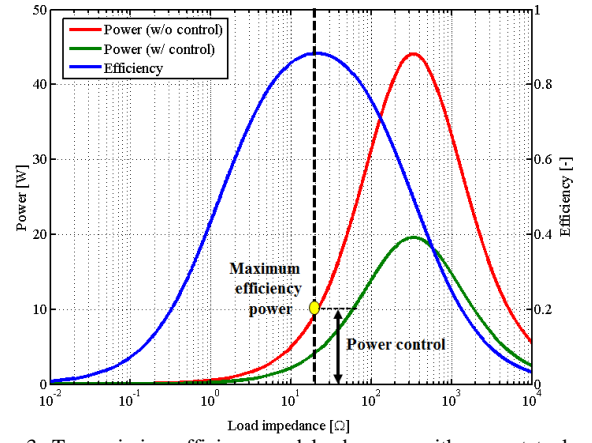


Figure 3: Transmission efficiency and load power with respect to load impedance for $V_1 = 20V$ and $L_m = 39.2 \mu H$.

short mode during the HAR switching period determines the amount of power received by the load.

Figure 4 shows how the control works and how the secondary side input parameters are shaped. In rectification mode, the rms value of secondary side voltage is unchanged, therefore the rms value of the secondary side input power P_2 is unchanged. The secondary side coil behaves like an equivalent current source so the current does not change as well. The power is calculated by averaging, as well as the efficiency; consequently, the averaged efficiency will be lower. In fact, during rectification mode the efficiency is maximum while in short mode it is zero since the load is not

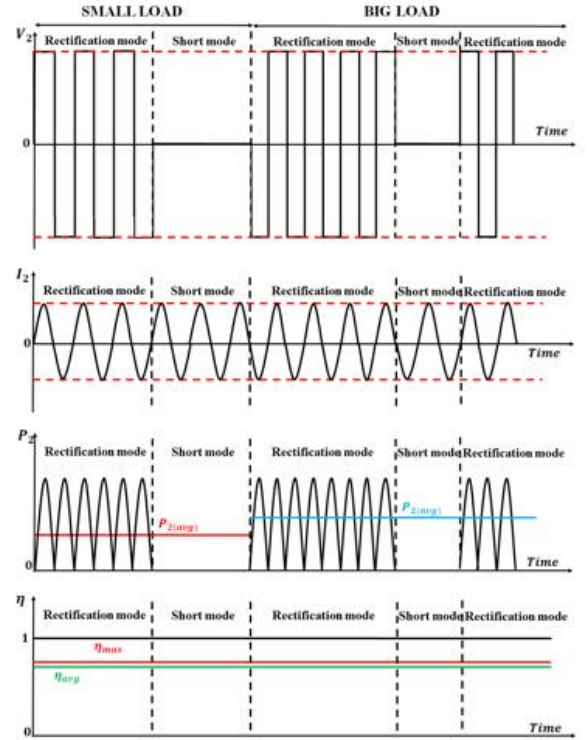


Figure 4: Control concept with parameters waveforms (top to bottom: HAR input voltage V_2 , HAR input current I_2 , HAR input power P_2 , total efficiency η).

supplied. The modulation is done via short mode: the longer it is, the lesser the power received by the load, the lesser the averaged efficiency. In short mode there are certainly losses in the secondary side coil due to the circulating current.

V. CONTROL OPERATION

A. Control overview

A control to achieve the desired power with high transmission efficiency was proposed in [10]; in this paper, a similar control is used. By modulating the HAR output power P_{DC} and the DC/DC converter input voltage V_{DC} it is possible to send the desired power with high efficiency. Therefore, the control circuit has two degrees of freedom. In figure 5 and figure 6 are represented the control blocks for the HAR and DC/DC converter, respectively. The feedback controller designed with the pole placement method.

The voltage V_2 is difficult to measure directly because is a high frequency square wave, but its value can be obtained by averaging the measured value or by deriving from the power in the DC side.

In this paper, the following conditions are assumed:

- 1) Primary side coil voltage, system frequency and mutual inductance are known and fixed. Furthermore, the primary side voltage is always bigger than the load voltage.
- 2) The HAR switching frequency is at least one order of magnitude slower than the DC/DC converter switching frequency.

B. Operating point of HAR

The HAR is set to modulate the power by adjusting the average power sent to the load. In order to do that, a voltage formula related to the desired power P_L^* and the maximum power is necessary. From (7), the above mentioned voltage is computed as follows:

$$V_{P_L^*} = V_{P_{\max}} - \sqrt{V_{P_{\max}}^2 - \frac{[R_1 R_2 + (\omega L_m)^2] P_L^*}{R_1}} \quad (8)$$

By rearranging (8), the value of the desired power as a function of the voltage is obtained as follows:

$$P_L^* = \frac{R_1 [V_{P_{\max}}^2 - (V_{P_L^*} - V_{P_{\max}})^2]}{R_1 R_2 + (\omega L_m)^2} \quad (9)$$

Since the aim is to achieve high transmission efficiency, the upper limit of the desired power is reached when $V_{P_L^*} = V_{\eta_{\max}}$; therefore, (9) becomes:

$$P_{L_{\max}}^* = \frac{R_1 [V_{P_{\max}}^2 - (V_{\eta_{\max}} - V_{P_{\max}})^2]}{R_1 R_2 + (\omega L_m)^2} \quad (10)$$

From (8) is possible to derive the duty cycle of the HAR. In fact, the duty cycle is proportional to the ratio between the input and output voltage of a converter. This is because their values depend on the conduction time over the time period. Therefore, the duty cycle of the HAR is given by:

$$D_{PWM} = \frac{\pi}{2\sqrt{2}} \frac{V_{P_L^*}}{V_{DC}} \quad (11)$$

Actually, the DC link voltage is controlled by the DC/DC converter and is set to the maximum efficiency value. Certainly, the time ratio between short mode and rectification mode is included in the value of the duty cycle.

C. Operating point of DC/DC converter

The DC/DC converter can be either a buck converter or a buck-boost converter, however in the current case of study a buck converter is considered. Therefore, since the control makes the DC link voltage equal to the maximum efficiency voltage, the duty cycle will be simply:

$$D_{DC/DC} = \frac{V_{DC}}{V_{load}} \quad (12)$$

Notice that both the load voltage and the DC link voltage are set to values that do not change or change very little, therefore the duty cycle of the DC/DC converter becomes nearly constant.

D. Influence of the converter switching frequency

The switching frequency plays an important role in the success of the control method. In fact, if both the HAR and the DC/DC converter had the same switching frequency, the control would not work at all because the two controllers would be operating in contrast to each other. By adopting condition 2), the two switching frequencies are different

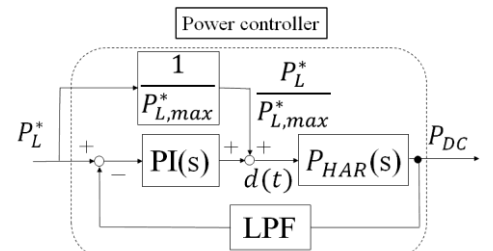


Figure 5: HAR power control block.

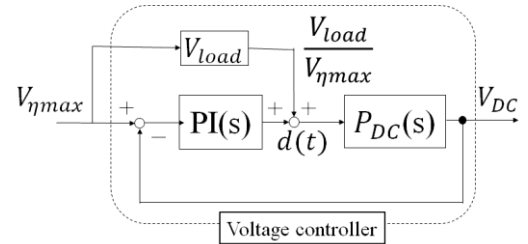


Figure 6: DC/DC converter DC link efficiency control block.

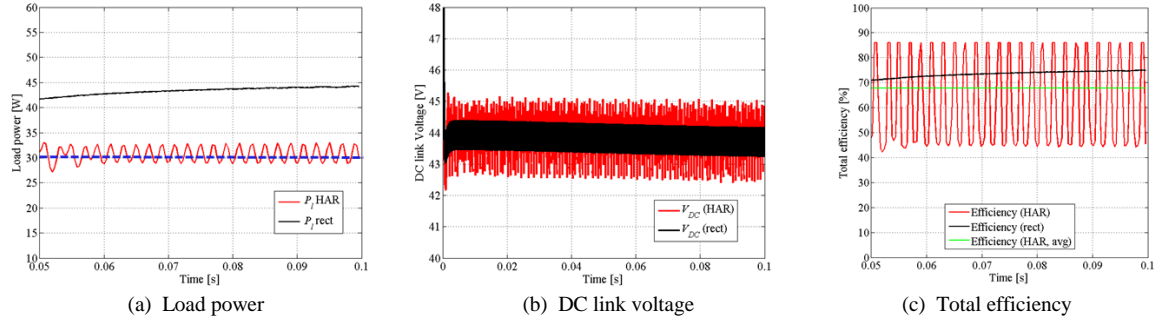


Figure 7: Simulation results in case A (primary side voltage $V_1 = 50V$ and reference power $P_{ref} = 30W$).

enough for the two controllers to work with minimal interference from each other.

VI. SIMULATION AND EXPERIMENTAL RESULTS

For different values of primary side voltage and power, the efficiency and power were measured to confirm the effectiveness of the proposed method. By changing the primary side voltage and reference power, also the maximum efficiency voltage and the maximum power voltage change as well. The mutual inductance is not changed. The DC/DC converter resistance R_{conv} and its inductance L_{conv} are 0.1Ω and 1 mH , respectively; as for the DC/DC converter filter capacitance, its value is 1 mF . The HAR switching frequency is set to 500 Hz , while the DC/DC converter switching frequency is 20 kHz .

A. Simulation results

The performance of the proposed system has been compared to the one of a conventional system composed by a full bridge diode rectifier and a DC/DC converter controlled with the same voltage regulator as figure 7. In the simulations, two cases have been considered:

- The primary side voltage is 50 V (peak value), the reference power is 30 W .
- The primary side voltage is 18 V (peak value), the reference power is 5 W .

In the case of a full bridge diode rectifier, the power sent to the load is fixed and cannot be changed; on the other hand, with the HAR it is possible to set a different power reference value and send it to the load.

The simulation results of case A are shown in figure 7. The red line corresponds to the HAR and DC/DC converter system, while the black line refers to the conventional rectifier and DC/DC converter system set up in maximum efficiency conditions. The control appears to work as expected, as the average DC link voltage coincides with $V_{\eta_{max}}$ and the load power ends up matching the power reference. The average efficiency of the proposed system is almost equal to the one of the conventional system set in maximum efficiency condition. However, the load power waveform is not smooth, as shown in figure 7(a): this is reflected on the efficiency plot, too, and the reason is that the HAR forces the input voltage V_2 to be zero by short mode in order to regulate the incoming power. This will be

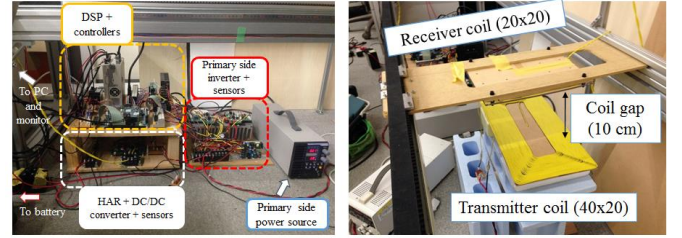


Figure 8: Experimental setup.

a problem when there is low load condition because the oscillations can be very big and therefore the average efficiency will be lower, as shown in figure 7(c); moreover, if the DC/DC converter is a buck-boost converter, during short mode the power flow could be reversed and the battery will power the DC link capacitor. This problem can be solved by putting a big enough DC link capacitance. Since the proposed system allows short mode and therefore not sending power to the load, in order to avoid discontinuous conduction mode of the DC/DC converter is necessary to take care in the design of the inductor, too.

The experimental parameters are close to the conditions of case B, therefore the simulation results of case B are shown along to the experimental results for a reliable evaluation of the proposed method.

B. Experimental results

The experimental setup is shown in figure 8. It includes a DC generator (TAKASAGO ZX-400LA), the primary side inverter, primary and secondary coils, a HAR, a DC/DC converter, a DSP (Myway PE-PRO/F28335A) and a battery as a load. As for DC values, there four sensors: two sensors are in the primary side, while the other are in the secondary side. Each side has a set composed of a voltage and current sensor: in the primary side the inverter input voltage and current is measured; on the other hand, the secondary side sensors measure the HAR output current and voltage. The experiment aim is to verify the robustness of the control by introducing a step change in the load reference power.

The simulation results of case B are shown in figure 9 while the experimental results are shown in figure 10. As it can be seen from 10(a), the power reference of the secondary side load varies as a step from 3 W to 5 W . The power changes to match effectively the reference. The primary power changes as well because the length of short

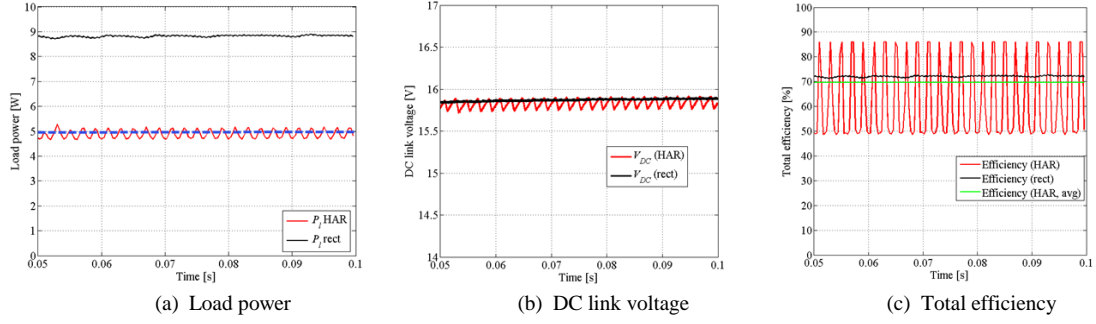


Figure 9: Simulation results in case B (primary side voltage $V_1 = 18\text{ V}$ and reference power $P_{ref} = 5\text{ W}$).

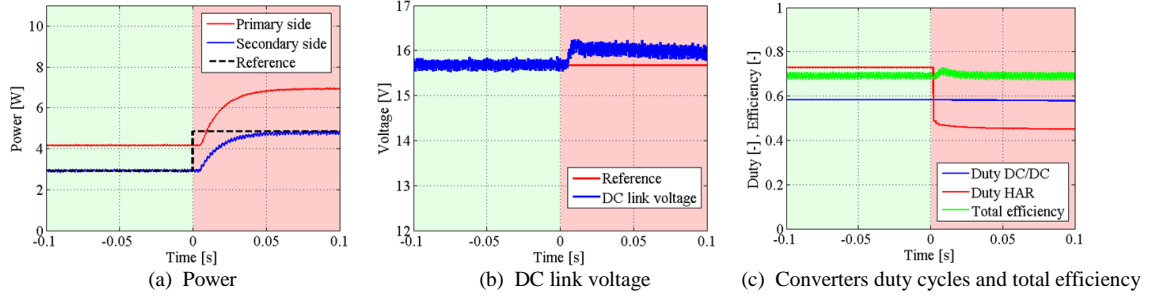


Figure 10: Experimental results with power reference step from 3 W to 5 W.

mode is reduced, therefore the average power becomes bigger. The slight delay in the reference matching, visible in all the graphics in figure 10, is due to the low switching frequency of the HAR. The DC link voltage changes slightly as in figure 10(b). After the step, the voltage is about 3% bigger than the reference. However, this does not affect much the control since the shift from the maximum efficiency value is negligible. In figure 10(c), only the HAR duty cycle changes while the DC/DC converter duty cycle is nearly unchanged. The duty cycle is referenced to the lower side of the converter. The averaged source to load efficiency agrees with the simulation results in 9(c): in fact, the averaged total efficiency in the experiment is 67.28% whereas in the simulation is 69.79%. The efficiency does not change with the power step, even though it increases during the transient.

VII. CONCLUSION AND FUTURE WORKS

This paper focused on the secondary side of a wireless power transfer system. The authors proposed a novel method performing both power control and efficiency control only on the secondary side, independently from the primary side, by using a HAR and a DC/DC converter. Simulations and experiments showed that the proposed control method is effective.

Future works include losses analysis, power surges mitigation control and the dynamic charging experiment.

REFERENCES

[1] A. Kurs, A. Karalis, R. Moffatt, J.D. Jannopoulos, P. Fisher, M. Soljacic, "Wireless power transfer via strongly coupled magnetic

resonances", Science Expressions on 7 June 2007, Vol. 317, No. 5834, pp. 83-86, 2007.

- [2] Siqu Li, Chunting Chris Mi, "Wireless power transfer for electric vehicle applications", IEEE Journal of Emerging and Selected Topics in Power Electronics, pp. 1-14, 2013.
- [3] H. L. Li, A. P. Hu, G. A. Covic, T. Chunsen, "A new primary power regulation method for contactless power transfer", IEEE International Conference on Industrial Technology (ICIT), pp. 1-5, 2009.
- [4] J. M. Miller, C. P. White, O. C. Onar, P. M. Ryan, "Grid side regulation of wireless power charging of plug-in electric vehicles", IEEE Energy Conversion Congress and Exposition (ECCE), pp. 261-268, 2012.
- [5] W. Chwei-Sen, O. H. Stielau, G. A. Covic, "Design considerations for a contactless electric vehicle battery charger", IEEE Transactions on Industrial Electronics, vol. 52, pp. 1308-1314, 2005.
- [6] M. Fu, C. Ma, X. Zhu, "A cascaded boost-buck converter for high efficiency wireless power transfer systems", IEEE Transactions on Industrial Informatics, Vol. 10, No. 3, pp. 1972-1980, 2014.
- [7] H.H. Wu, A. Gilchrist, K. D. Sealy, D. Bronson, "A high efficiency 5 kW inductive charger for EVs using dual side control", IEEE Transactions on Industrial Informatics, vol. 8, pp. 585-595, 2012.
- [8] T. Diekhans, R. W. De Doncker, "A dual-side controlled inductive power transfer system optimized for large coupling factor variations" IEEE Energy Conversion Conference and Exposition (ECCE) 2014, pp. 652-659, 2014.
- [9] K. Hata, T. Imura and Y. Hori, "Maximum Efficiency Control of Wireless Power Transfer Considering Dynamics of DC-DC Converter for Moving Electric Vehicles", The Applied Power Electronics Conference and Exposition, pp. 3301-3306, 2015
- [10] T. Hiramatsu, X. Huang, M. Kato, T. Imura and Y. Hori, "Wireless Charging Power Control for HESS Through Receiver Side Voltage Control", The Applied Power Electronics Conference and Exposition, pp. 1614-1619, 2015.
- [11] M. Kato, T. Imura, Y. Hori, "New characteristics analysis considering transmission distance and load variation in wireless power transfer via magnetic resosnat coupling", IEEE Proceedings INTELEC, 2012.
- [12] M. Kato, T. Imura, Y. Hori, "Study on maximizing efficiency by secondary side using DC-DC converter in wireless power transfer via magnetic resosnat coupling", EVS27, pp. 1-5, 2013.